

# MARINE PILING ACOUSTICS MODELLING BY USE OF WAVE EQUATION ANALYSIS

M Wood            University of Southampton, Southampton, UK  
V Humphrey      University of Southampton, Southampton, UK

## 1 INTRODUCTION

The UK is currently the world leader in energy produced from offshore wind with an installed capacity of 2.9 GW<sup>1</sup>. It is envisaged that the UK could generate 18 GW by 2020, with the possibility of deploying over 40 GW by 2030<sup>2</sup>. The majority of this power is due to be generated from The Crown Estate's Round 3 programme, which comprises the development of nine offshore wind farms around the UK<sup>3,4</sup>. The typical capacity of a single wind turbine is 5-7 MW, with larger capacity turbines being developed<sup>3</sup>. Therefore it is likely that many thousands of wind turbines will be installed in UK waters in the coming years to meet these targets.

Marine piling is commonly used in the construction of offshore wind farms<sup>5</sup>. This involves using a ram, with a mass in the region of 100 tonnes, repeatedly impacted against the top of a steel tubular cylindrical pile that may be up to 6 m in diameter and many tens of metres in length<sup>5</sup>. This impacting process has been found to generate high-level acoustic disturbances (greater than 210 dB (re 1  $\mu$ Pa) peak-to-peak at 57 m) that may then propagate to large distances<sup>6</sup>. There is increasing concern that this noise may adversely affect marine life<sup>7</sup>. Consequently there is interest in being able to predict the noise generated by these operations.

A variety of methods have been used to model the pile acoustics in recent years<sup>8-12</sup>. Typically the pile has been modelled in situ, most often comprising a linear elastic pile situated in a homogeneous fluid sediment. The energy input into the pile is used to overcome side shaft friction and plastically deforming the soil such that the pile is driven into the sediment. Frictional losses between the pile and the sediment have been included in some models by use of a complex sound speed in the sections of pile in contact with the soil<sup>8,9</sup>. An alternative is to use an empirically-derived reflection coefficient to represent energy losses at each end of the pile<sup>13</sup>.

The analysis and modelling of wave propagation down the driven pile is not new; methods have been developed over many years that model the stress wave down the pile taking measurable soil properties into account. The most frequent method of predicting the ultimate capacity of piles involves using dynamic formulae relating it to pile set (vertical displacement of the pile per hammer blow)<sup>14</sup>; this approach is known as Wave Equation Analysis of Piles (WEAP). This paper presents work based on this method to determine the pile motion that is then used as an input to an acoustic model.

Section 2 introduces a typical WEAP program, with an overview of the inputs and outputs of such a model, and a comparison against a standard finite-element approach. Section 3 presents a simple acoustic model and the results of coupling the two models to produce a wave-field. The results and findings are discussed in Section 4, with avenues of future work outlined in Section 5.

## 2 WAVE EQUATION ANALYSIS OF PILES

### 2.1 Motivation for using WEAP models

During the planning stages of the pile installation, studies are undertaken to ensure the drivability of a pile<sup>14</sup>. This process allows the engineer to determine the most appropriate hammer configuration, and ensures that the pile will not be subject to excessive stresses that may cause damage. These studies typically involve the use of a WEAP program. The analysis involved is based on solving the one-dimensional wave equation taking the internal forces and motions of the pile elements into consideration<sup>15</sup>. The primary outcome of this approach is to determine the relationship between the ultimate pile load or capacity and the pile set. However, as part of the process, a time history of the motion of the pile is also calculated; this is of more interest to the acoustical engineer.

It is proposed that the pile compression calculated from the one-dimensional problem could be used, along with Poisson's ratio, to calculate the radial expansion of the pile. The radial expansion of the pile may then be used as an input to an acoustical model to generate the sound field. Furthermore, the axial motion of the sediment directly adjacent to the pile may be used as an input to model the outgoing shear waves. The advantage in taking this approach is that the pile-sediment interface is more realistically modelled, and that this technique has been refined and used in the civil industry for many years.

### 2.2 WEAP model overview

The problem is defined by the one-dimensional wave equation of the form

$$\frac{\partial^2 Z(z, t)}{\partial t^2} = \frac{E}{\rho} \frac{\partial^2 Z(z, t)}{\partial z^2} \pm R(z, t) \quad (1)$$

where  $Z$  is the axial displacement of a point in the pile from its original position,  $E$  is the Young's modulus of the pile,  $\rho$  is the density of the pile,  $t$  is time,  $z$  is position along the vertical axis and  $R$  comprises all soil resistance terms. The use of this form of the equation implies that displacements are restricted to the axial direction only and consequently only axisymmetric solutions are possible.

Due to the nature of the soil resistance terms, a solution typically cannot be found by analytical methods. Instead, a finite-difference model is created involving splitting the pile into a one-dimensional series of masses, springs, and dampers. Where the pile is in contact with the sediment, the system is coupled to a separate mechanical system comprising a spring, damper, and plastic slider. The idealised system is shown in Figure 1. The ram is included in the idealisation as a mass with an initial downward velocity determined by the hammer energy rating, mass, and efficiency<sup>15</sup>. The force of the hammer is transmitted to the pile through a capblock represented by a spring; this spring allows no tensile forces to be transmitted representing the possible separation of the ram and the capblock.

Although the problem in Equation 1 could be solved numerically, it has been shown that the problem can be defined by a series of five simpler equations. These equations may be solved iteratively for each element and for each time step<sup>15</sup>. This form of the problem is the most commonly adopted method in pile-driving analysis<sup>15</sup>. A program based on these five equations has been written in MATLAB and has been used to generate the results for this paper.

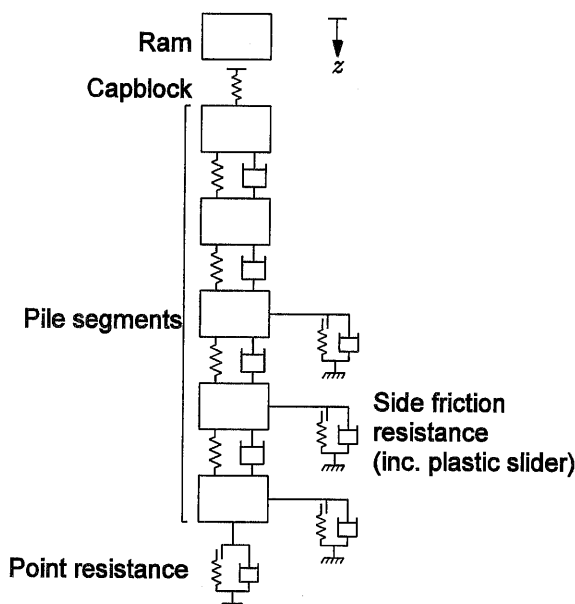


Figure 1. The idealised pile model. The pile itself is decomposed into a series of masses interconnected with springs and dampers. The soil is represented by connected sub-systems comprising a spring, a damper, and a plastic slider.

## 2.3 Model inputs and outputs

The analysis was performed for a 50 m long pile, 6 m outer diameter with a wall thickness of 65 mm. The pile was embedded 20 m into the sediment prior to the modelled strike, and the water depth was 20 m. The energy rating for the hammer was 2300 kJ, and the ram mass was 115000 kg; assuming 100% efficiency, this gave an impact velocity of  $6.32 \text{ ms}^{-1}$ . The sediment has been modelled as 'dense sand' with skin friction value of 75 kPa and an end bearing value of 12 MPa. These friction values along with the soil quake (allowable soil deformation before it reaches the elastic limit) provide values for the stiffnesses of the soil springs of  $2.78 \times 10^8 \text{ Nm}^{-1}$  for the side springs and  $5.73 \times 10^9 \text{ Nm}^{-1}$  for the point spring. The pile itself is made of steel with a density of  $7850 \text{ kgm}^{-3}$ , a Young's modulus of 205.8 GPa, and a Poisson's ratio of 0.28. The WEAP program was run with a time step of  $40 \mu\text{s}$  (effective sampling frequency of 25 kHz) up to a maximum time of 0.14 s. Considering a maximum frequency of 1000 Hz, and a 'rod' wavespeed in the pile of  $5120 \text{ ms}^{-1}$ , the minimum wavelength would be 5.12 m. To provide at least ten points per wavelength the length of each pile element was set at 0.5 m; no benefit was seen for increasing the axial resolution beyond this value. On an Intel quad-core i7 processor machine running at 3.40 GHz the run took 4.35 seconds to complete.

The WEAP model calculates the element displacement, compression, force between elements, soil resistance, and the resulting element velocity for each point in time. The radial expansion of the pile as a function of time can be inferred from the local compression of the pile. The radial expansion,  $x$ , is given by

$$x = \frac{\nu DC}{\delta L}, \quad (2)$$

where  $\nu$  is Poisson's ratio,  $D$  is the diameter of the pile,  $C$  is the compression, and  $\delta L$  is the length of a single pile element.

## 2.4 Comparison with other models

The equivalent run was performed using IHCWAVE Stress Wave Program<sup>17</sup>, and in COMSOL multiphysics finite-element program for both fluid and solid sediments; all parameters were kept the

same where possible. In the case of the COMSOL models the force input at the top of the pile was generated using an analytical solution for the hammer<sup>11</sup>. The sediment had a density of  $1900 \text{ kgm}^{-3}$ , and a compressional sound speed of  $1625 \text{ ms}^{-1}$ . Additionally, in the solid sediment model, the sediment shear wave speed was  $110 \text{ ms}^{-1}$  which is consistent for sand at 1 m depth<sup>16</sup>. In IHCWAVE, the driving mode was set to 'Redrive after full setup', with all other parameters as for the WEAP model.

Figure 2 shows the pile toe displacement as a function of time for the discussed WEAP model, the IHCWAVE Stress Wave Program, and the two COMSOL finite-element models. This highlights the pile motion differences between the approaches. The plastic deformation allowed in the WEAP model and IHCWAVE dissipates system energy and consequently both settle rapidly at a defined pile set. However, the solid-sediment finite-element model simply oscillates close to its initial value due to being held in place by the sediment, whilst the fluid-sediment model shows the pile descending step-wise with each reflection of the pulse; this step-wise motion reaches 20 cm by 0.1 s.

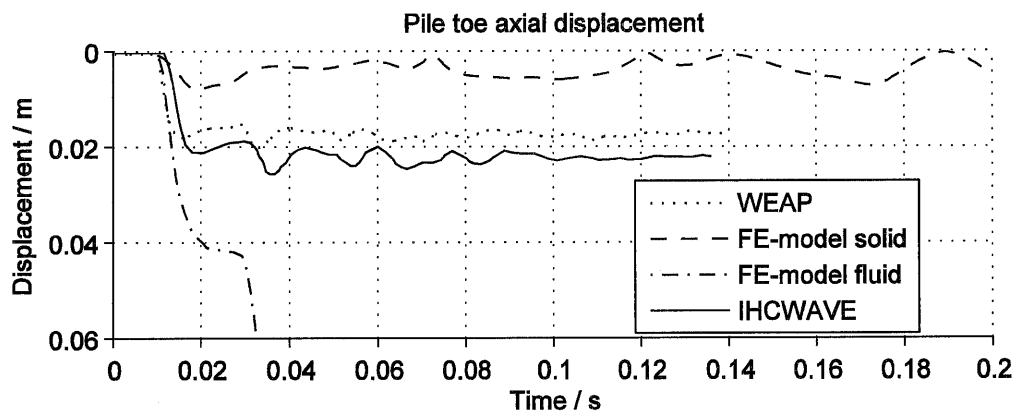


Figure 2. The modelled pile toe displacement for the four models. The WEAP model and IHCWAVE results are characteristically similar, with the effects of the first and second pulses clearly visible at approximately 0.02 s and 0.035 s. The finite-element model with the elastic soil continues to oscillate beyond the time taken for the other models to settle. The fluid-soil model features a continuous step-wise descent which reaches 20 cm depth by 0.1 s.

### 3 COUPLED RESULTS

From the WEAP model, one may determine the radial velocities of each point of the pile as a function of time. To provide an illustration of the possible acoustic field emanating from the pile this has been coupled to a ring-source model assuming that each point in the pile can be treated as an ideal dipole-source with no other pile-boundary interactions. Additionally, the medium at all points below the water surface is assumed to be water; the air-water interface is modelled as a perfect pressure-release boundary.

A single ring is shown diagrammatically in Figure 3. This shows a number of dipoles on a ring of radius  $a$ . One can consider a single dipole on the ring and a receiver constrained to the  $xz$  plane as indicated in Figure 4; here, the source position is at  $S = [S_x, S_y, 0]$ ,  $R = [R_x, 0, R_z]$ , and  $\phi$  is the angle between the direction of the dipole and the direction from  $S$  to  $R$ . The acoustic pressure due to a dipole source may be written as

$$p(r, \phi) \propto \frac{\cos(\phi)}{r} e^{-jkr}, \quad (3)$$

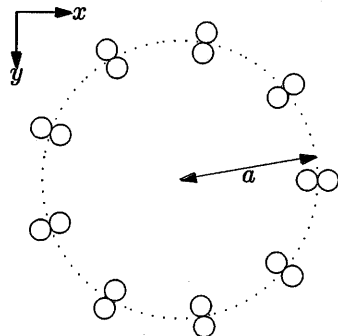


Figure 3. A diagrammatic representation of the dipole ring source

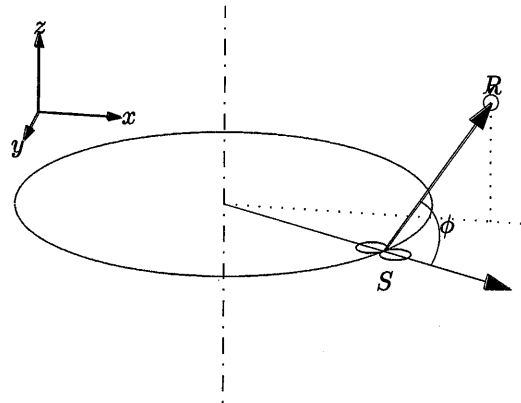


Figure 4. Geometry source a single dipole source at  $S$  and receiver  $R$ .

where  $r$  is the distance between the source and the receiver. Introducing  $\mathbf{A} = \mathbf{R} - \mathbf{S}$  as the vector from the source to the receiver (i.e.  $r = |\mathbf{A}|$ ), and using standard vector geometry one obtains

$$\mathbf{A} \cdot \mathbf{S} = |\mathbf{A}| |\mathbf{S}| \cos \phi, \quad (4)$$

and thus Equation 3 can be written as

$$p \propto \frac{\mathbf{A} \cdot \mathbf{S}}{|\mathbf{A}|^2 |\mathbf{S}|} e^{-jk|\mathbf{A}|}. \quad (5)$$

To generate the result for an entire ring of sources, one notes that  $\mathbf{S} = [a \cos \theta, a \sin \theta, 0]$  and sums the sources over the range  $0 \leq \theta < 2\pi$ , such that for a single receiver point  $\mathbf{R}$  the pressure is

$$p(\mathbf{R}) \propto \int_{\theta=0}^{2\pi} \frac{(\mathbf{R} - \mathbf{S}(\theta)) \cdot \mathbf{S}(\theta)}{|\mathbf{R} - \mathbf{S}(\theta)|^2 |\mathbf{S}(\theta)|} e^{-jk|\mathbf{R} - \mathbf{S}(\theta)|} d\theta, \quad (6)$$

which can be solved using standard numerical techniques.

Each axial element of the pile is assumed to represent an individual ring source. The Fourier transform of the radial velocity of each point in the pile is calculated to provide an amplitude and phase for all frequencies. The ring source field is generated for each frequency; each one is then convoluted in space with the pile velocities to provide a complete field at the single frequency. An image-source model is used in order to provide results from the reflection from the water. An inverse Fourier transform then provides the time domain representation of the field.

Figure 5 shows the wave-field produced using this method at 0.02 s after impact. The wavefront caused by the first down-going pulse is clearly seen, closely followed by the contribution from the opposite side. Further wavefronts, however, have much reduced amplitudes due to the loss of energy into the sediment. The angles of the conical waves are as expected, and agree well with previous work<sup>12</sup>. These angles are due to the relative wavespeeds of the pulse down the pile and in the water.

The received pressure as a function of time at a single point is shown in Figure 6. The point is taken close to the pile such that there is little acoustic influence from the sediment. The wavefronts from the first down-going pulse are most prominent; two peaks are seen due to the contribution from the near-side and the far-side of the pile wall. Beyond this, initially the pressure exhibits a rapid attenuation but is then followed by a longer decay.

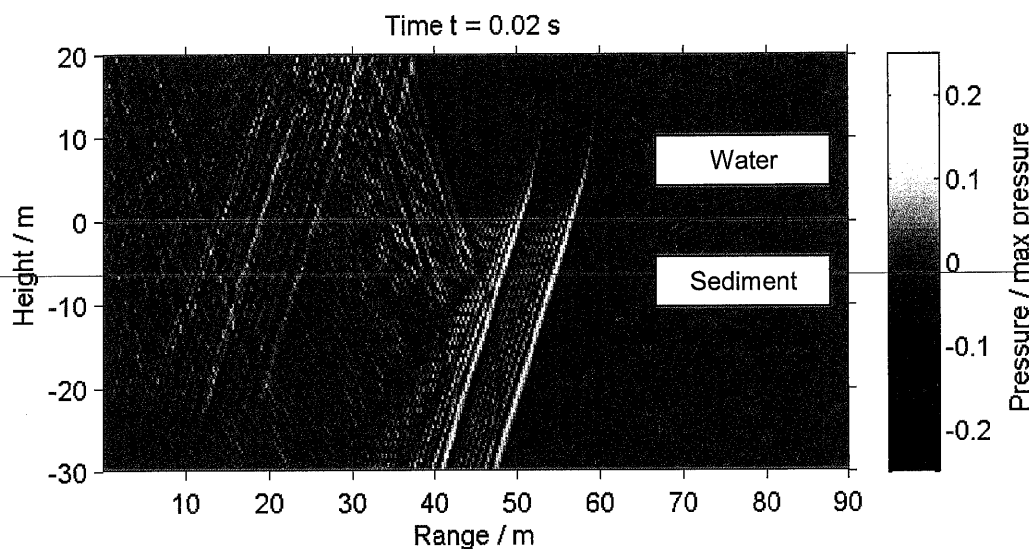


Figure 5. Radial slice of the wave-field calculated using the WEAP model coupled with the ring-source model. The wave generated by the first down-going pulse is clearly visible. Subsequent wavefronts are significantly reduced in amplitude. Due to discussed acoustic model limitations the wave does not reflect off the water-sediment interface nor is attenuation included in the sediment.

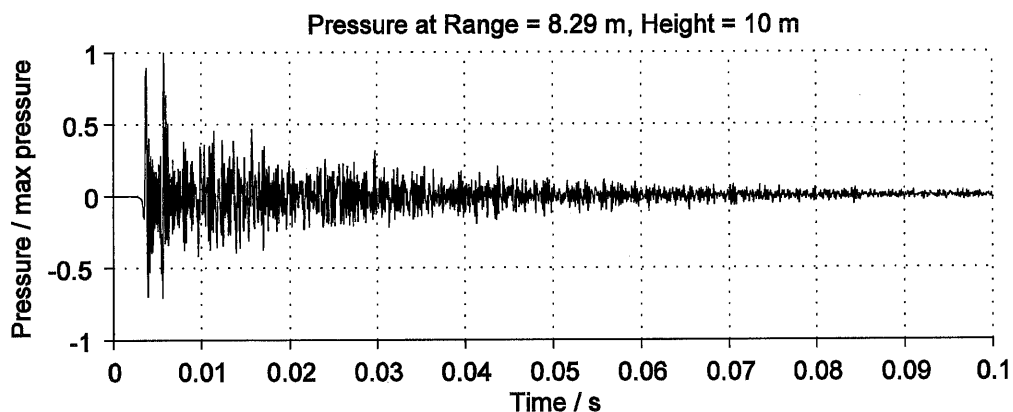


Figure 6. The received pressure at a point 5.29 m from the pile wall at mid-depth in the water column. Acoustic model limitations are avoided as at this position in the wave-field there is little acoustic influence from the sediment. The first pulse from both walls dominate the signal, with initial rapid attenuation followed by a longer decay.

This is a very simple model designed to picture the possible results of incorporating the WEAP results into an acoustic model. There is no special consideration of the sediment, and in this case it is treated exactly the same as water. This leads to the pressures to be greater in the sediment than one would otherwise expect due to no loss from reflections at the water-sediment interface and there being no attenuation in the sediment. Another shortcoming of the model is that each dipole is based on the free-field greens function rather than include any influence from the pile itself. Despite the limitations, however, the coupling provides useful insight into the wave generation process and supports the argument for using WEAP models for pile-driving acoustics.

## 4 DISCUSSION

This paper demonstrates the use of a WEAP program being incorporated in an acoustic model of pile-driving noise. The WEAP model provides a more realistic representation of the pile motion following striking than the finite-element model examples due to the treatment of the sediment interface. Unless specifically taken into account, the effect of the sediment in finite-element models may provide misleading results; it has been shown that the pile toe displacement is greatly affected by how the sediment is treated. The advantages of the WEAP model are that the approach has been honed over many years of use in industry, and is also typically quick to run making it suitable for parametric studies.

A simple acoustic model that demonstrates how the outputs from the WEAP program can be used has also been presented. This provides a qualitative example that is in agreement with what is known about noise from pile driving. A more sophisticated model could also take into account proper treatment of the sediment with reflections at the interface and allow for shear wave propagation.

It is documented that the most significant portion of the noise produced by piling is contained in the first wavefront<sup>13</sup>. This is generated before the pulse down the pile reaches the sediment, and thus is not affected by the sediment model. However, there is concern that the contribution from the subterranean portion is significant particularly when considering mitigation methods that comprise a barrier in the water column. It is for this reason that the pile motion below the sediment-sea interface needs to be realistically modelled, especially for greater driving depths where a significant proportion of the sound will have been generated in this region.

## 5 FUTURE WORK

As discussed, there are significant areas of development for this model. With regards to the WEAP model itself, the current sediment mechanical subsystem provides no distinction between the radiation damping and the viscous damping provided by the soil. A more sophisticated model has been suggested that takes each into account separately<sup>14</sup>. Additionally, the radiation damping from the water in this case has been omitted; this should be included as there is a small effect on the pile wave due to the slight change in impedance.

Currently the acoustic model exists only to illustrate aspects of the WEAP model and its applicability to pile acoustics. It is envisaged that the results from this model be used as an input to a finite-element model in order to model the acoustic aspect. This would allow for a quantitative comparison against other models and against recorded results.

## 6 ACKNOWLEDGEMENTS

The author would like to acknowledge the support and funding from the National Physical Laboratory, the Engineering and Physical Sciences Research Council, and the Faculty of Engineering and the Environment at the University of Southampton.

## 7 REFERENCES

1. RenewablesUK. UK offshore wind continues to surge ahead! Retrieved from <http://www.renewableuk.com/en/news/press-releases.cfm/uk-offshore-wind-continues-to-surge-ahead>. (2013).

2. The Department of Energy and Climate Change. UK Renewable Energy Roadmap. London: Crown copyright. Retrieved from <http://www.decc.gov.uk/assets/decc/11/meeting-energy-demand/renewable-energy/2167-uk-renewable-energy-roadmap.pdf>. (2011).
3. The Crown Estate. UK Offshore Wind Report 2012. London: The Crown Estate. Retrieved from [http://www.thecrownestate.co.uk/media/297872/UK\\_offshore\\_wind\\_report\\_2012.pdf](http://www.thecrownestate.co.uk/media/297872/UK_offshore_wind_report_2012.pdf). (2012).
4. The Crown Estate. Offshore Renewable Energy (UK). London: The Crown Estate. Retrieved from <http://www.thecrownestate.co.uk/media/266431/offshore-renewable-energy-uk.pdf>. (2013).
5. The Crown Estate. A Guide to an Offshore Wind Farm. London: The Crown Estate. Retrieved from [http://www.thecrownestate.co.uk/media/211144/guide\\_to\\_offshore\\_windfarm.pdf](http://www.thecrownestate.co.uk/media/211144/guide_to_offshore_windfarm.pdf). (2010).
6. Nedwell, J., & Howell, D. A review of offshore windfarm related underwater noise sources (p. 63). Retrieved from <http://www.subacoustech.com/information/downloads/reports/544R0308.pdf>. (2004).
7. Popper, A. N., & Hastings, M. C. The effects of anthropogenic sources of sound on fishes. *Journal of fish biology*, 75(3), 455–89. (2009).
8. Zampolli, M., Nijhof, M. J. J., De Jong, C. A. F., Ainslie, M. A., Jansen, E. H. W., & Quesson, B. a J. Validation of finite element computations for the quantitative prediction of underwater noise from impact pile driving. *The Journal of the Acoustical Society of America*, 133(1), 72–81. (2013).
9. Zampolli, M., De Jong, C. A. F., Ainslie, M. A., Jansen, E. H. W., Quesson, B., Fillinger, L., Middeldorp, F., et al. Quantitative predictions of pile driving noise , modelling approaches and open issues. Hamburg: Federal Maritime and Hydrographic Agency (BSH) - Workshop: "Standards on Underwater Noise." (2011).
10. Wood, M. A., & Humphrey, V. Numerical modelling of offshore impact piling by use of normal modes. *MARNAV 2012: International Conference on Advances and Challenges in Marine Noise and Vibration*. Glasgow. (2012).
11. Wood, M. A., & Humphrey, V. Dependence of radiated piling noise on the hammer cushion properties. *Proceedings of the 11th European Conference on Underwater Acoustics* (pp. 585–590). Edinburgh: Institute of Acoustics. (2012).
12. Reinhall, P. G., & Dahl, P. H. Acoustic radiation from a submerged pile during pile driving. *OCEANS 2010* (pp. 1–4). Seattle, Washington, USA: IEEE. (2010).
13. Dahl, P. H., & Reinhall, P. G. Observations of underwater sound from impact pile driving using a vertical line array. *Proceedings of the 11th European Conference on Underwater Acoustics* (pp. 1340–1347). Edinburgh: Institute of Acoustics. (2012).
14. Zienkiewicz, O. C., Pastor, M., Chan, A. H. C., Xie, Y. M., Seed, R. B., Duncan, J. M., Ou, C. Y., et al. *Advanced Geotechnical Analyses*. (P. K. Banerjee & R. Butterfield, Eds.). Foundations. Barking, UK: Elsevier Science Publishers Ltd. (1991).
15. Poulos, H. G., & Davis, E. H. Pile foundation analysis and design (p. 408). John Wiley & Sons Inc. (1980).
16. Jensen, F. B., Kuperman, W. A., Porter, M. B., & Schmidt, H. *Computational Ocean Acoustics* (2nd ed.). New York, NY: Springer New York. (2011).
17. van Foeken, R. IHCWAVE Stress Wave Package Ver 1.3. TNO, Netherlands. (2001).